

FROZEN MARTIAN LAHARS? EMPLACEMENT MECHANISMS AND GEOLOGIC IMPACT OF UTOPIA-ELYSIUM FLOWS. G. B. M. Pedersen^{1,2} and James W. Head³. ¹Nordic Volcanological Center, Institute of Earth Sciences, University of Iceland, Sturlugata 7, 101 Reykjavík, Iceland. ²Department of Earth Sciences, University of Aarhus, Hoegh-Guldberggade 2, 8000 Aarhus C, Denmark (grobirkefeldt@gmail.com). ³Department of Geological Sciences, Brown University, Providence, RI 02912 USA.

Introduction: Lahar is defined as a general term for an event during which a water-rock-debris mixture (different than a normal stream flow) flows rapidly from a volcano [1]. Morphologically, volcanoclastic deposits originating from terrestrial lahars often have channeled deposits in the center incising terraces of different elevations [e.g., 2,3]. These medial deposits are flanked by marginal levees and lobes, which together with arcuate surface ridges, reflect the unstable, surging nature of lahars.

On Mars both dike [4-6] and sill [7,8] intrusions have been proposed as mechanisms for generating major lahars (in various regions such as Mangela Valles, Elysium Fossae, Cerberus Fossae and Athabasca Valles) either by melting substantial amount of ground ice [8-12] or by cracking the cryosphere allowing drainage of confined aquifers [4-6, 13]. However, little focus has been placed on the emplacement properties of lahars under martian conditions, though martian temperature and pressure may have had a significant impact on the lahar emplacement and morphology.

Based on regional high-resolution data from the CTX camera (6m/pixel) this study investigates the emplacement mechanisms of the proposed mega lahars in the Utopia-Elysium region [5,9-11] and how they affected the subsequent geologic development in the area.

Geologic setting: The study area is centered around Hrad Vallis and encompasses the northwestern part of the Elysium rise, the western part of Galaxias Chaos and the transition into Utopia Planitia (138°-145°E; 31°N-40°N) (Fig. 1).

A variety of volcano-ice interactions have been proposed in the transition zone between Elysium volcanic province and Utopia Planitia. Immense outflow channels originating on the northwest of the Elysium rise extend more than a thousand kilometers into Utopia Basin and have termini that are spread over a vertical range of > 1500m [10, 14]. These outflow deposits have been interpreted as evidence for mega-lahars due to their lobate morphology, well-defined snouts, and close association with channels [9-11] and have been suggested to be of Early Amazonian age [12, 15]. Other evidence for ice-volcano interactions has been reported ranging from pseudocraters [16]; mud-like deposits thought to be caused by phreatomagmatic explosions due to sills intruding an ice-rich subsurface [8]

and associated thermally distinct craters (probably resulting from interaction between a hot mudflow and ground ice [17]). Subglacial volcanic edifices such as table mountains [18] and möberg ridges [19-21] have also been reported.

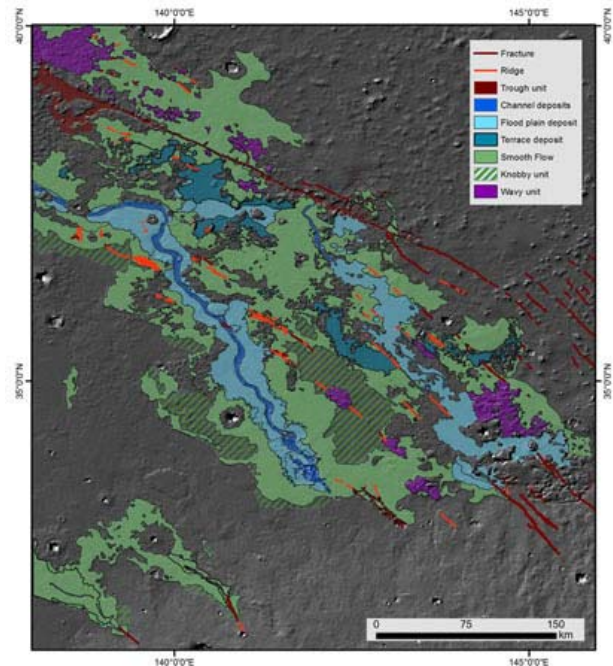


Figure 1. Study area and distribution of morphologic units (SF, CD, FPD, TD, KU, WU, TU), ridges (red) and fractures (dark red).

Morphology and Distribution: Various units have been interpreted to relate to volcano-ice interactions and include (Fig. 1): smooth flow, *SF* (green, ~45,400 km²); channel deposit, *CD* (blue, ~1,890 km²); flood plain deposit, *FPD* (light blue, ~13,730 km²); terrace deposit, *TD* (turquoise, ~4,200 km²); knobby unit, *KU* (shaded green, ~8,550 km²); wavy unit, *WU* (purple, ~4,900 km²); trough unit, *TU* (brown, ~4,000 km²); and ridges (red) and fractures (dark red). *SF* is the most extensive deposit with diagnostic steep, lobate flow fronts with upward convex snouts (Fig. 2), variable thickness (10-100m), enclosed depressions pits and hollows, crenulated rims and internal fractures. Distinct crater morphologies are observed resembling ring-mold craters (RMCs) [22-23], thermally distinct craters [17] and ice-cauldron-like features [21].

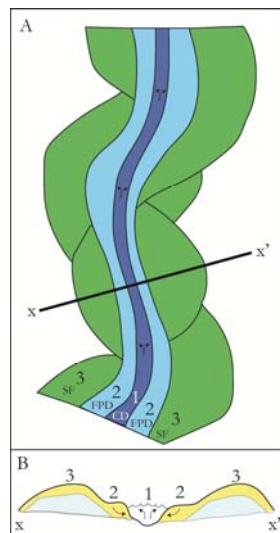
CD, *FPD* and *TD* are recognizable by their very flat, smooth appearance and normal impact craters.

Both FPD and TD display flow-like textured albedo variations, while CD is associated with very characteristic tear-drop shaped islands.

KU is characterized by its knobby surface and its gradual stratigraphic relationship with *SF*, and *WU* consists of 17 irregular elongated low sloping edifices trending NW-SE, 130-250m high with wavy-smooth-surface, normal craters and an irregular outline with raised rims.

Emplacement of flows and geologic impact: *CD*, *FPD*, and *TD* resemble fluvial landforms and are morphologically very different from *SF*. However, all four deposits are closely related stratigraphically and originate abruptly at approximately -3750m elevation in association with ridges, fractures and troughs, which suggest that all four deposits result from the same type of process. The observations support the lahar hypothesis put forward by previous workers [5,9-11] and suggests that the proximal, medial and distal deposits of the outflow deposits have very diverse morphologies that can be explained by varying degrees of water drainage and freezing. Regular channel and flood plain deposits are found in the central part of the outflow deposits (*CD*, *FPD* and *TD*), whereas the distal and marginal deposits (*SF*) are interpreted to contain significant amounts of ice because of their distinct morphological properties. Figure 2 (modified from Fig. 2 in [5]) illustrates this concept where the marginal lobes (no. 3 in Fig. 2) of the lahar deposit are ice-rich whereas the medial channels and flood plain deposits (no. 1 and 2 in Fig. 2) are ice-poor due to drainage. The cross-section in Figure 2B envisions how outflow material moved from the central part of the flows to the margins, creating overbank deposits and individual lobes of material similar to terrestrial lahars. However, unlike terrestrial lahars, the water within these slower moving, overbank flows froze due to the cold martian

Figure 2. Sketch of lahar deposition where (A) shows a plan view and (B) display a cross section at x-x'. No. 1 marks the medial channel (channel deposit, *CD*, dark blue), no. 2 marks the flood plain deposit (*FPD*, light blue) and no. 3 is lobes of smooth flow (*SF*, green) consisting of an ice-poor top layer (yellow in fig. 2B) with an ice-cemented core (white in fig. 2B).



conditions, creating an ice-rich deposit, while the central parts of the flow created channel and flat flood plain deposit similar to terrestrial systems. The morphologic properties and stratigraphic relations between *SF* and *KU*, *WU*, ridges and fractures imply that subsequent volcanic activity interacted with the ice-rich deposits and modified the *SF* deposits by deflation, and post-depositional remobilization. The morphologies related to sub-lahar intrusions of the frozen lahar deposits include; 1) Seventeen ridges that are interpreted to be möberg ridges (due to their NW-SE orientation, distinct ridge-crests and association with fractures and linear ridges), and 2) depressions with nested faults interpreted to be similar to terrestrial ice-cauldrons, which form by enhanced subglacial geothermal activity including subglacial volcanic eruptions.

Conclusions: This study support the lahar hypothesis by previous workers. However, there is morphologic evidence that lahar emplacement under martian conditions only drain in the central parts, whereas the water in the distal parts of the outflow deposit (~75% of the total outflow deposit in the Galaxias region) freezes, resulting in a double-layered deposit consisting of ice-rich core with an ice-poor surface layer. It is furthermore suggested that continued near-surface intrusive igneous activity was highly affected by the presence of the ice-rich lahar deposits, generating ground-ice-volcano interactions resulting in a secondary suite of ice-volcano morphologies.

References: [1] G. A. Smith and W. J. Fritz (1989) *Geology* 17, 375-376. [2] J.-C. Thouret et al. (1998) *Bull. Volcanol.* 59, 460-480. [3] L. M. Tanarro et al. (2010) *Geomorphology* 122, 178-190. [4] L. Wilson and J. W. Head (2002) *JGR* 107, 1-24. [5] P. Russell and J. Head (2003) *JGR* 108, 18-11. [6] J. W. Head et al. (2003) *GRL* 30, 1-4. [7] L. Wilson and J.W. Head (1994) *Rev. Geophys.* 32, 221-263. [8] L. Wilson and P. J. Mouginis-Mark (2003) *JGR* 108, E8, 5082, 1-16. [9] E. Christiansen (1989) *Icarus* 17, 203. [10] E. Christiansen and R. Greeley (1981) *LPSC XII*. [11] E. H. Christiansen and J. A. Hopley (1986) *LPSC XVII*, 125-126. [12] K. L. Tanaka et al. (1992) USGS. Misc. Invest. Ser., Map I-2147. [13] D. M. Burr et al. (2002) *Icarus* 159, 53-73. [14] M. A. Ivanov and J.W. Head (2001) *JGR* 106, E2, 3275-3295. [15] K. L. Tanaka et al. (2005) USGS. Misc. Invest. Ser., Map I-2811. [16] P. J. Mouginis-Mark (1985) *Icarus* 64, 265-284. [17] A. R. Morris & P. J. Mouginis-Mark (2006) *Icarus* 180, 335-347. [18] C. Allen (1979) *JGR*, 84, 8048. [19] M. Chapman (1994) *Icarus* 109, 393-406. [20] M. Chapman et al. (2000) in: Zimbelman, J. R., Gregg, T. K. P. (Eds.) *Environmental effects on volcanic eruptions - from deep oceans to deep space*, Kluwer Academic/Plenum Publishers, New York, 39-72. [21] G.B. M. Pedersen et al. (2010) *EPSL* 294, 4247-439. [22] A. Kress and J. W. Head (2008) *GRL* 35, L23206. [23] G. B. M. Pedersen and J. W. Head (2010) *PSS* 58, 1953-1970.